

## ANN Modeling in Pb(II) Removal from Water by Clay-Polymer Composites Fabricated via the Melt-Blending

Derrick S. Dlamini, Ajay K. Mishra, Bhekile B. Mamba

Department of Applied Chemistry, University of Johannesburg, Doornfontein 2028, Johannesburg, Gauteng, South Africa

Correspondence to: B. B. Mamba (E-mail: bmamba@uj.ac.za)

**ABSTRACT:** This work presents two new related aspects in heavy-metal adsorption. The first aspect is the use of Cloisite<sup>®</sup> C20A-polycaprolactone (C20A-PCL) composite with the aid of dry Na<sub>2</sub>SO<sub>4</sub> in Pb(II) extraction from water. The composite was fabricated by means of the melt-blending method at a filler loading rate of 3% (w/w). This material was able to remove 87% of Pb(II) from water despite the fact that the polymer is a thermoplastic and the C20A is hydrophobic. The second aspect is the modeling of the adsorption data obtained using polymer-clay composites synthesized via the melt-blending method by artificial neural networks. A network with 10 neurons and using TRAINLM, and employing tansig function in the input layer and purelin in the output layer was found to be optimal. The network was used to predict the adsorption efficiency of Pb(II) by several clay-polymer composites and the correlation was satisfactory. © 2013 Wiley Periodicals, Inc. *J. Appl. Polym. Sci.* 130: 3894–3901, 2013

**KEYWORDS:** adsorption; amorphous; applications; clay; composites

Received 16 October 2012; accepted 11 June 2013; Published online 2 July 2013

DOI: 10.1002/app.39656

### INTRODUCTION

Because of the sustained and rapid increase in industrialization worldwide, the pollution of water cannot be eliminated but could be minimized by controlling the waste generation. Once the water has been polluted, it should be cleaned. Every individual and company is obligated by international laws to avoid environmental pollution to protect aquatic life. Furthermore, the big challenge facing governments nowadays is the scarcity of clean water available for household consumption. One of the biggest challenges in water treatment is that each pollutant has a unique chemistry hence it needs specialized treatment. It is for this reason that much research has been done in this field and that a large number of publications have been produced for the common water pollutants like Pb(II). Even though, a huge amount of work has been done on the removal of Pb(II) from water using adsorption,<sup>1–7</sup> a lot of research work is still being undertaken using newly developed adsorbents. Every research study on the adsorption of Pb(II) from aqueous environments is generally targeted at producing chemically and thermally stable adsorbents, reproducible adsorbents, and high adsorption efficiency. These ambitious research projects have seen the introduction of polymer composites for use in water treatment.<sup>1,8–11</sup>

Polymer composite materials are generally made of two or more components containing a polymer as a matrix. Clay-polymer composites are common in water treatment because of the adsorptive properties of the clay. Clay-polymer composites can be

easily recovered after adsorption, unlike powder adsorbents like activated carbon. The performance of the composites as an adsorbent can be affected by the fabrication technique used because a synthesis method is selected based on the chemical and/or physical properties of the polymer to be used, among other factors. There are three methods widely used in the preparation of clay-polymer composites: solution blending, melt-blending, and *in situ* polymerization.<sup>12–14</sup> The melt-blending method uses thermoplastic polymers. Unfortunately such polymers are usually hydrophobic. However, the hydrophobic polymers are essential in preparing water-stable materials. Water-stable adsorbents can be regenerated and reused through adsorption/desorption experiments, thus reducing the operating costs.

An ideal water-treatment procedure should be compatible with engineering tools for optimum control and management. Artificial neural networks (ANN) have been successfully applied in recent years, especially to water-treatment systems. ANN is a data-based method for modeling that can present mathematical functions for both linear and nonlinear systems.<sup>15</sup> Neural networks (NN) are based on mapping input vectors and the corresponding target vectors during training until it can approximate a function that associates the input vectors with the specific output vectors. In addition to curve fitting, NN can be used as pattern recognition, clustering, and dynamic time-series tools. In curve-fitting mode, once a network has been created and configured, it should be trained, validated and tested. During

training, the weights and biases of the network are iteratively tuned to lessen the error between the input and the output. The weights and biases can be adjusted manually or automatically. ANN have been successfully applied in the environmental engineering field like heavy-metal removal from water using different adsorbents.<sup>16,17</sup> Since, a network is created and configured relative to the data set being used, it is important that every special material (adsorbent) be given a particular focus for investigation.

In the present study, we proposed a two-layer ANN model using a feed-forward propagation algorithm for modeling Pb(II) adsorption by polymer-clay composites. An optimization study to determine the optimal number of neurons, data distribution, and transfer function was done and the model was used to predict the effects of selected adsorption parameters, namely initial concentration of Pb(II) ions, initial pH, and temperature. This study is important because the stability (thermally and chemically) and ease of recovery of polymer composites developed using the melt-blending method of composite synthesis suggests that these materials could be the next generation of adsorbents in water treatment. Studies like this one are expected stimulate interest in integrating polymer-nanocomposite strips in real water treatment to improve adsorbent recovery. A computer-simulated model like ANN is necessary in developing an automated wastewater-treatment plant to lower the operating cost of the treatment plant.

## MATERIALS AND PROTOCOL

### Fabrication of Composites

The composites were fabricated with ethylene vinyl acetate (EVA) with 10% VA (Plastamid, Johannesburg, South Africa), and polycaprolactone (PCL) (Aldrich Chemicals, Johannesburg, South Africa) as the matrices. Cloisite<sup>®</sup> 20A (C20A) (Southern Clay Products, TX) and Bentonite Ocean MD (MD) (G&W Minerals, Wadeville, South Africa) clays were used as the filler. Since the polymers are hydrophobic, dry sodium sulfate (15% w/w) was used to improve water permeation. A Thermo Scientific HAAKE Rheomex OS equipped with roller-type rotors coupled with a single-screw extruder was used in the melt-blending method. The fabrication was done in a mixing chamber with a volume of 64 cm<sup>3</sup>; a temperature set at 100°C; a rotational speed of 60 rpm; and a residence time of 30 min. The composites were then chopped into small chips, which were fed into the extruder to obtain strips. The composite strips were soaked in 1000 ml of deionized water for 24 h with vigorous stirring to remove leachable Na<sup>+</sup> and SO<sub>4</sub><sup>2-</sup> ions. The physical properties of these composites were reported and discussed in our previously published work.<sup>8,9</sup>

### Data Collection

The C20A-PCL composite was used to remove Pb(II) from water using Pb(NO<sub>3</sub>)<sub>2</sub> as a source of Pb(II) ions. Batch-adsorption experiments were conducted to establish the optimum pH, contact time, initial concentration, and the effect of temperature on the uptake of Pb(II). The adsorbent weight was 20 mg and the volume of the analyte solutions was about 20 ml. The initial pH of the solution was adjusted using 0.1M KOH or HCl. After adsorption the solutions were analyzed for

any remaining Pb(II) concentration using atomic adsorption spectroscopy (AAS) operated at a wavelength of 283.3 nm with a corresponding slit width of 0.5 nm. The performance of the adsorbents in Pb(II) extraction from water is reported in adsorption efficiency (R(%)), which was calculated using the following relation:

$$R(\%) = 100 \times \left( 1 - \frac{C_t}{C_0} \right) \quad (1)$$

where C<sub>0</sub> and C<sub>t</sub> are the initial concentration and the concentration at time *t*, respectively.

To enlarge the quantity of data to satisfy the ANN creation and configuration, the Pb(II) adsorption data collected using C20A-EVA, MD-EVA, and MD-PCL as adsorbents<sup>8,9</sup> were used.

### ANN Software

In this study, the training, validation and testing of the ANN model was carried out using the Neural Network Toolbox<sup>™</sup> on MATLAB 7.11.0 (R2010b) mathematical software. A two-layer feed forward neural network (NN) with purelin transfer function in the output layer was used. The adsorption efficiency was chosen as the output, and 100 experimental data points obtained using C20A-EVA, MD-EVA, C20A-PCL, and MD-PCL composites as adsorbents were used to feed the network.

## RESULTS AND DISCUSSIONS

### Optimizing Network

**Network Architecture.** As mentioned in the previous sections, a two-layer feed-forward NN network with a single hidden layer was used in this study. To fully define the network architecture, the number of neurons was optimized based on the mean square error (MSE), which can be calculated by the following equation:

$$MSE = \frac{1}{N} \sum_{i=1}^N (y_{i, \text{actual}} - y_{i, \text{predicted}})^2 \quad (2)$$

where *y<sub>i, actual</sub>* and *y<sub>i, predicted</sub>* are the experimental and predicted adsorption efficiencies, respectively

*N* is the number of number of data points.

The results in Figure 1 show that 1 neuron had the highest MSE (5.834) among the number of neurons selected. Increasing the number of neurons from 1 to 2 slightly decreased the MSE to 4.795. The lowest MSE (0.00748) was found when the number of neurons is 10.

The MSE initially decreased with an increase in the number of neurons until a minimal was reached at 0.00748 and increased thereafter. A similar observation was reported by Ghandehari et al.<sup>18</sup> in their work on modelling crossflow microfiltration using ANN and Yetilmezsoy et al.<sup>16</sup> where they were modeling Pb(II) adsorption from aqueous solutions by *Antep pistachio* shells. The increment at higher neuron numbers can be ascribed to the characteristics of the MSE performance index and the input vector used.<sup>16</sup> On the basis of these results, 10 neurons in the hidden layer were considered optimal.

**Effect of Learning Algorithm.** The learning algorithm is another parameter that deserves attention because different learning

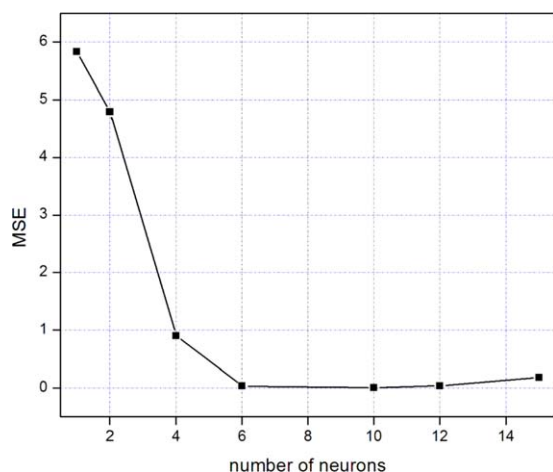


**Figure 1.** Variation of the number of neurons with MSE.

algorithms can produce a network with different accuracy towards specific data. The Levenberg-Marquardt (TRAINLM), Powell-Beale Restarts (TRAINCGB), Fletcher-Reeves Update (TRAINCGF), and Quasi-Newton (TRAINBFG, TRAINOSS) learning algorithms were tested through trial and error to discover the best performing algorithm for the data used in this study. The best algorithm was selected based on regression ( $R^2$ ) value and MSE. The results are summarized in Table I.

A good training algorithm should have a high  $R^2$  but a small MSE. The TRAINLM learning algorithm had the highest  $R^2$  values, ranging from 0.9997 to 1.000, and TRAINOSS algorithm had the lowest values. These results clearly indicate that TRAINLM is the best training system for the data used in this study. Turana et al.<sup>19</sup> found TRAINLM to be the optimum learning algorithm in modeling the biosorption of Zn(II) from leachate.

**Effect of Transfer Function.** There are three transfer functions used in creating and configuring a network. These are: log-sigmoid (logsig), tan-sigmoid (tansig), and purelin. The logsig function generates outputs between 0 and 1 as the neuron's net input goes from negative to positive infinity as shown by the following equation:

$$f(x) = \frac{1}{1 + e^{-x}} \quad (3)$$

On the other hand, the tansig function generates outputs between  $-1$  and  $1$  as can be deduced from the following equation:

$$f(x) = \frac{2}{1 + \exp(-2x)} - 1 \quad (4)$$

Occasionally, the linear transfer function purelin is used and it lets the network produce values outside the range  $-1$  to  $+1$ . This function is mostly used in the output layer but in the present study it was tested in the input layer because the performance of these functions can be influenced by the data used. The three training functions were used with the purpose of finding the best function for the modeling of Pb(II) removal from water using polymer-clay composites synthesized via the melt-blending method. In all the networks, the purelin function was used in the output layer. The results (shown in Table II) are reported in terms of MSE and  $R^2$ .

The network trained with the tansig function had the lowest  $R^2$  (0.9999) and the lowest MSE values (0.0069). When the purelin function was used in the input layer, the  $R^2$  was the lowest at 0.9864 and the MSE was highest at 15.52. On the basis of these results, the tansig function was selected as the best for training the network. After the optimization tests, a two-layer network with 10 neurons in the hidden layer and tansig function in the input was adopted for modeling the adsorption of Pb(II) using polymer-clay composites fabricated using the melt-blending method.

**Effect of Data Distribution.** ANN is a data-based modeling tool. The set of data is divided into three categories: training, validation, and testing data. The amount of data in each of these categories can have an effect on the performance of the network, yet most studies have ignored this fact. The partitioning of the samples is reported in percentages. Unless otherwise specified, a network contained 3 inputs, 10 hidden layers, and 1 output.

From these results, it can be seen that varying the training data from 60% to 80% did not change the training accuracy as  $R^2$  stood at 1.000 in all the cases (Figure 2). The network with 10% validation data gave the highest validation  $R^2$  (1.0000). In the test data, 10% and 15% gave  $R^2 = 1.0000$  while 20% showed the lowest  $R^2$  (0.99556). The ideal data partitioning was identified by the  $R^2$  of the total (overall) process; hence 70 : 15 : 15 was found to be the optimum distribution ratio for the data used in the model. This decision was supported by the MSE for the 3 models: 0.0093 (80 : 10 : 10), 0.0072 (70 : 15 : 15), and 0.0348 (60 : 20 : 20).

#### Network Application

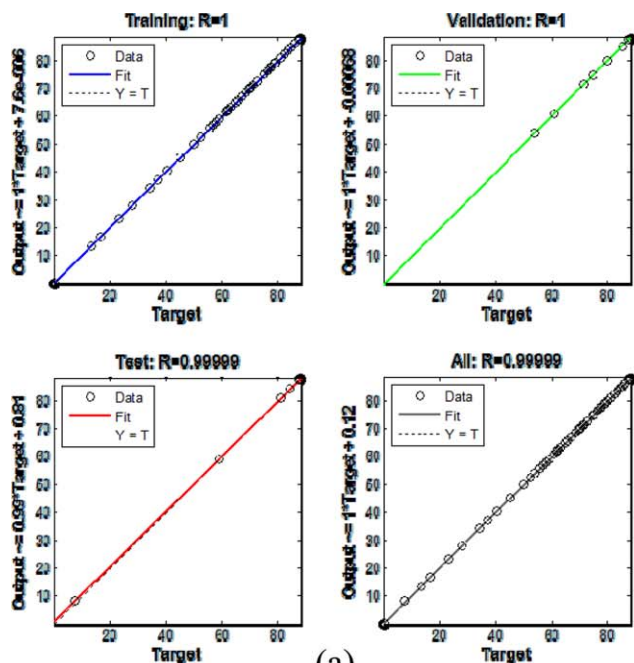
The optimal network designed to model the adsorption of Pb(II) from water using polymer-clay composites was tested in

**Table I.** Performance Evaluation of Network Based on Training Algorithm

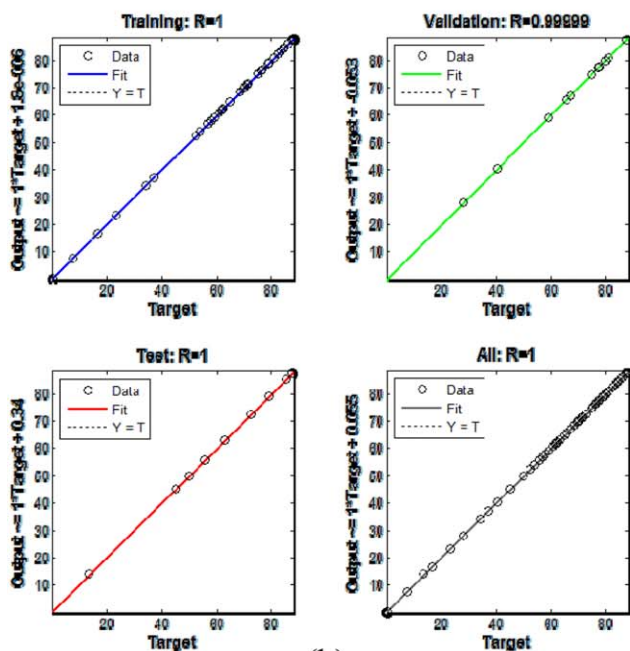
	Learning algorithm				
	TRAINLM	TRAINBFG	TRAINOSS	TRAINCGB	TRAINCGF
Train	1.000	0.9963	0.7479	0.9997	0.9980
Validation	1.000	0.9928	0.8317	0.9959	0.9989
Test	0.9997	0.9990	0.7908	0.9996	0.9984
Total	0.9999	0.9954	0.7590	0.9996	0.9981
MSE					
Total	0.0077	20.28	292.1	0.5412	1.393

**Table II.** Performance Evaluation of Network Based on Training Function

	Transfer function		
	Logsig	Purelin	Tansig
$R^2$	0.9996	0.9864	0.9999
MSE	0.0552	15.52	0.0069



(a)



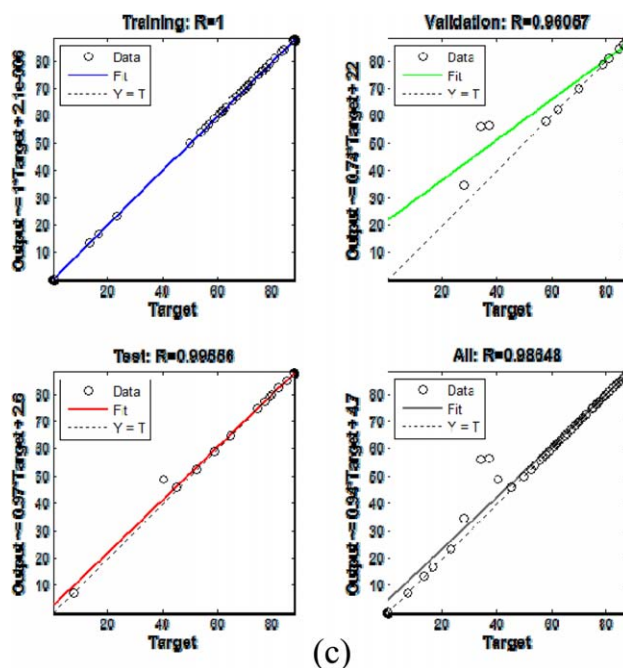
(b)

modeling the adsorption of Pb(II) in water by EVA-C20A, EVA-MD, PCL-C20A, and PCL-MD composite. Experimental data used for this purpose were obtained by varying the contact time, that is, the adsorption contact time was the input. The agreement between the experimental and predicted adsorption efficiency is depicted in Figure 3.

In this work, the accuracy of the ANN to predict the adsorption efficiency was based on  $R^2$ . As it can be seen from Figure 3, the lowest  $R^2$  is 0.9998 and the highest  $R^2$  is 1.000. This suggests that there is a high correlation between the actual and the predicted adsorption efficiency indicating that the network was configured well. It is obvious that the ANN is suitable for modeling the adsorption of Pb(II) on clay-polymer composites fabricated via the melt-blending technique. The network was then used to model the new adsorption results. These results were obtained using C20A-PCL as an adsorbent.

### Adsorbent Performance

To the best of our knowledge, the C20A-PCL composites fabricated via the melt-blending technique have never been used in water treatment. The C20A-PCL composite prepared in this work was tested for the removal of Pb(II) from water. As mentioned in “Fabrication of Composites Section,” dry sodium sulfate was used to enhance the water permeability in the composite. It is important that water penetrate the composite with considerable ease because the composites are 0.5 mm thick, which means that at 3% (w/w) filler content there would be few clay particles on the surface of the composite. Another reason for using this salt was that the melt-blending procedure applied in this work involved blending and extruding. The force applied during extrusion can result in a tight composite. The clay possesses the adsorption active sites and the polymer is just a support; it is therefore vital that the analyte solution penetrate



(c)

**Figure 2.** Data distribution (train: validate: test): (a) 80 : 10 : 10; (b) 70 : 15 : 15; and (c) 60 : 20 : 20. [Color figure can be viewed in the online issue, which is available at [wileyonlinelibrary.com](http://www.wileyonlinelibrary.com).]

**Figure 2.** (Continued)



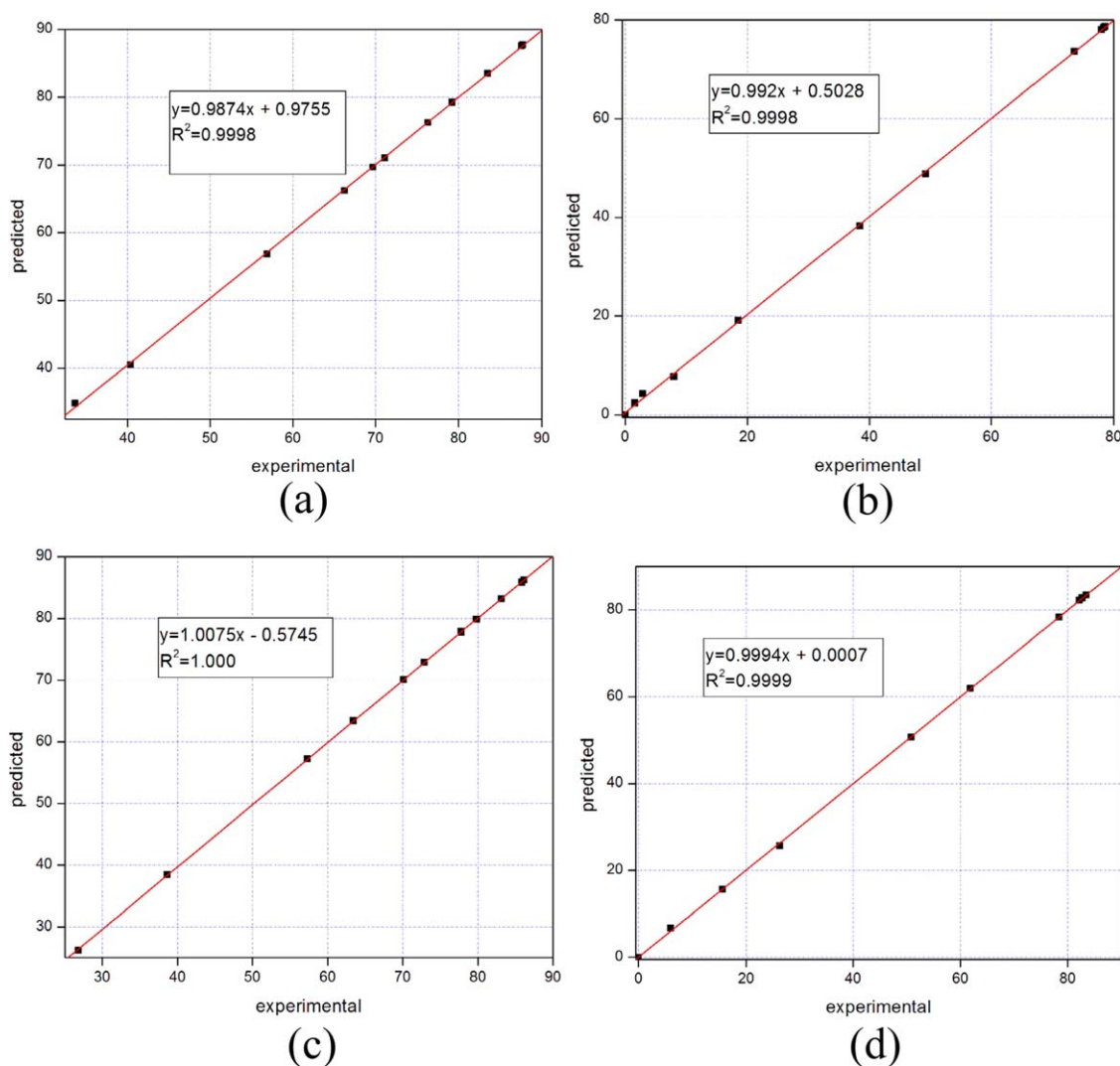


**Figure 3.** Correlation between predicted adsorption efficiency and the adsorption efficiency for: (a) EVA-C20A; (b) EVA-MD; (c) PCL-C20A; and (d) PCL-MD composites. [Color figure can be viewed in the online issue, which is available at [wileyonlinelibrary.com](http://wileyonlinelibrary.com).]

the composite favorably so that the Pb(II) ions are exposed to almost all the active sites.

**Effect of pH.** The hydrogen-ion potential (pH) is an adsorption parameter that needs special consideration. The pH determines the surface charge of adsorbents and the polarity of the adsorbents has an impact on adsorption efficiency. At lower pH the analyte solution would have a high concentration of hydrogen ions in the form of hydronium ( $H_3O^+$ ) ions. In the event the adsorbent is a nucleophile (e.g., bentonite clay) and the adsorbate is an electrophile (e.g., Pb(II)), the hydronium ions could compete for adsorption sites with the analyte. The high concentration of  $H_3O^+$  ions could also obstruct the movement of the adsorbate towards the adsorbent through repulsion, thereby limiting contact between the adsorbent and the adsorbate. Under higher pH conditions, there would be a high concentration of hydroxyl ( $-OH$ ) ions and they will complex with ions such as Pb(II).<sup>20</sup> The effect of pH on the uptake of Pb(II) from aqueous solutions using C20A-PCL composites is shown in

Figure 4. The experimental adsorption efficiency is compared with the adsorption efficiency predicted using the ANN model.

At low pH (pH 1–5.5), the adsorption efficiency increased as a result of the strong attraction that exists between the hydronium ions and the adsorbent leading to repulsion of Pb(II) ions.<sup>8</sup> At a pH of above 5.5, there is an increase in the adsorption efficiency. This observation can be ascribed to the disappearance of free Pb(II) ions in the solution due to interaction with the hydroxyl groups. The optimum pH for the adsorption of Pb(II) occurs at pH 5.5.<sup>8,9</sup>

**Effect of Contact Time.** The variation of the adsorption efficiency with the contact time is shown Figure 5. This figure shows that the adsorption reached equilibrium after 6 h with a maximum adsorption efficiency of 87%. This is remarkable considering that the matrix (PCL) of the composite is hydrophobic. The correlation between the experimental data and the data predicted using the ANN model is impressive.

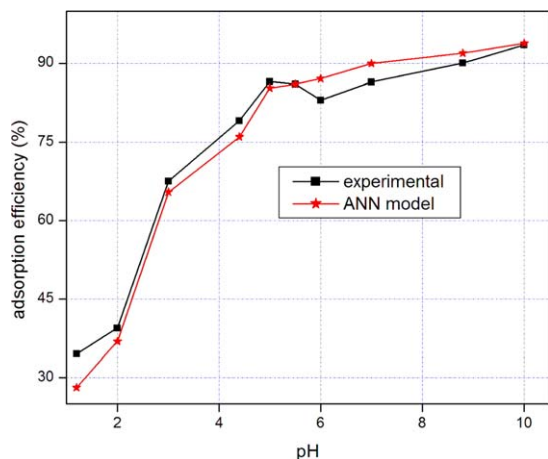


**Figure 4.** Effect of pH on the adsorption of Pb(II) using PCL-C20A composite at an initial concentration of 200 mg/l and  $T = 20^{\circ}\text{C}$ . [Color figure can be viewed in the online issue, which is available at [wileyonlinelibrary.com](http://wileyonlinelibrary.com).]

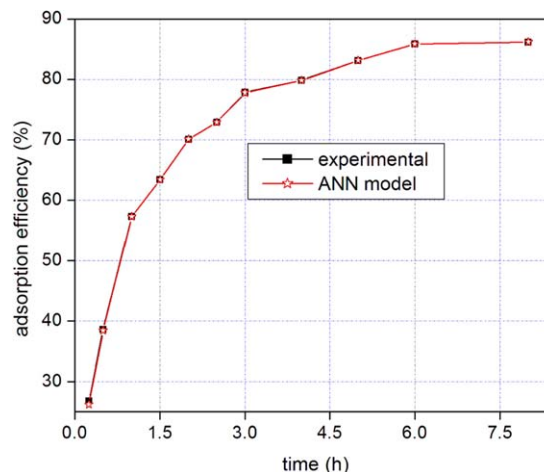


**Figure 5.** Adsorption kinetics of Pb(II) on PCL-C20A at pH 5.5,  $C_0 = 200$  mg/l, and  $T = 20^{\circ}\text{C}$ . [Color figure can be viewed in the online issue, which is available at [wileyonlinelibrary.com](http://wileyonlinelibrary.com).]

To understand how the amount of adsorbed metal changes with time, kinetic models were applied. The pseudo-first-order and the pseudo-second-order models are widely used for this purpose. The pseudo-first-order equation is given as follows:<sup>2</sup>

$$\log(q_e - q_t) = \log(q_e) - \frac{k_1}{2.303} t \quad (5)$$

where  $q_e$  is the adsorption capacity at equilibrium;  $q_t$  is the adsorption capacity at time  $t$ ;  $k_1$  is the first-order rate constant

Kinetic parameters of this model were calculated from the slope of the linear plot of  $\log(q_e - q_t)$  versus  $t$ . The second-order equation is given as follows:<sup>2</sup>

$$\frac{t}{q_t} = \frac{1}{k_2 q_e^2} + \frac{t}{q_e} \quad (6)$$

where  $k_2$  is the second-order rate constant

If the second-order kinetics is applicable, then the plot of  $t/q_t$  against  $t$  should show a linear relationship.

The plots are shown in Figure 6. From this figure, it is seen that the pseudo-first-order model has the lowest  $R^2$  value as compared to the pseudo-second-order model. The  $R^2$  suggests that pseudo-second-order model is suitable to describe the adsorption of Pb(II) onto the C20A-PCL.

**Effect of Temperature: Thermodynamic Studies.** The effect of temperature ranging from 303 to 343 K on the performance of the C20A-PCL composite in the extraction of Pb(II) initial concentration of 200 mg/L from water at pH 5.5 was investigated. The experimental results are compared with the ANN predicted results in Figure 7. Evidently, increasing the temperature from 303 to 328 K resulted in an increase in the adsorption efficiency from 88% to 91%. A further increase to 343 K caused an aggressive decrease in the percentage of Pb(II) adsorbed to 82%. A similar trend was reported by Yetilmesoy et al.<sup>16</sup> on their work on Pb(II) adsorption from aqueous solution by *Antep pistachio*.

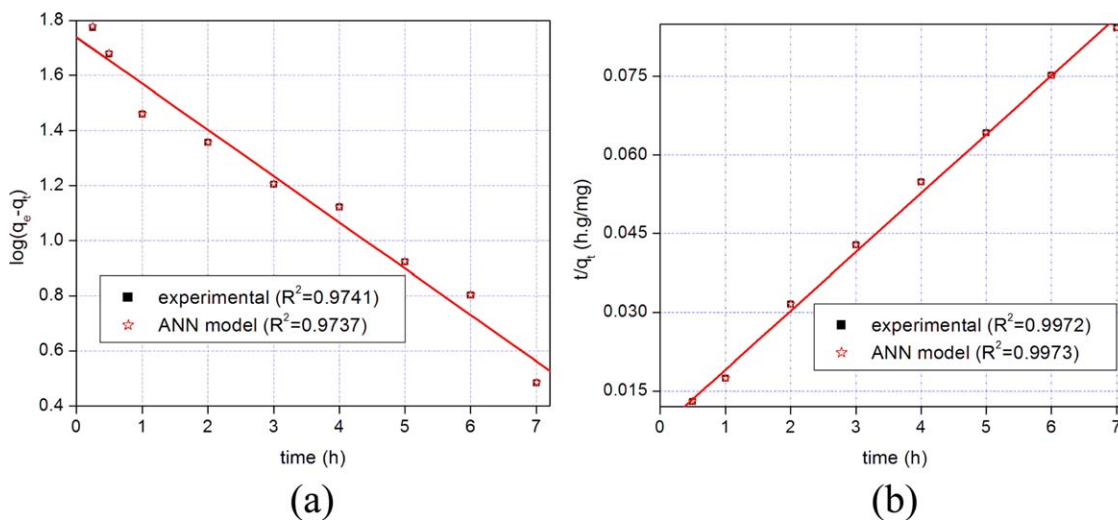


**Figure 6.** Kinetic models: (a) pseudo-first-order; and (b) pseudo-second-order. [Color figure can be viewed in the online issue, which is available at [wileyonlinelibrary.com](http://wileyonlinelibrary.com).]

**Table III.** Thermodynamic Parameters

T (K)	$\Delta G^{\circ}$ (KJ mol <sup>-1</sup> )	$\Delta H^{\circ}$ (KJ mol <sup>-1</sup> )	$\Delta S^{\circ}$ (J mol <sup>-1</sup> K <sup>-1</sup> )
303	30.82		
318	36.76	-13.82	-55.18
328	37.61		

The concept of adsorption is based on the “collision” between the adsorbate and the adsorbent. The observed increase in adsorption efficiency can be attributed to an increase in the mobility of the ions. It is generally accepted that at higher temperatures, molecular interaction forces (both chemical and physical) are weakened and this explains the decrease in the amount of Pb(II) adsorbed at  $T = 70^{\circ}\text{C}$ . To obtain a deeper insight into the effect of temperature on the uptake of Pb(II) by the C20A-PCL composite, the thermodynamic feasibility of the study was determined by using the thermodynamic parameters: free Gibbs energy ( $\Delta G^{\circ}$ ), enthalpy ( $\Delta H^{\circ}$ ), and entropy ( $\Delta S^{\circ}$ ).  $\Delta G^{\circ}$  was computed using the following relation:

$$\Delta G^{\circ} = -RT \ln K_c \quad (7)$$

where  $R$  is the gas constant ( $8.314 \text{ J mol}^{-1} \text{ K}^{-1}$ );  $T$  is temperature (K);  $K_c$  is the apparent equilibrium constant ( $K_c$ ) of the adsorption and is defined in terms of the Pb(II) adsorbed at equilibrium ( $C_{\text{ads}}$ ), and the equilibrium Pb(II) concentration ( $C_e$ ) and can be calculated by the following equation<sup>21</sup>:

$$K_c = \frac{C_{\text{ads}}}{C_e} \quad (8)$$

The values of  $\Delta H^{\circ}$  and  $\Delta S^{\circ}$  were calculated from the slope and intercept of the plot of  $\ln K_c$  versus  $1/T$ .<sup>21</sup>

$$\ln K_c = \frac{\Delta S^{\circ}}{R} - \frac{\Delta H^{\circ}}{RT} \quad (9)$$

Equation (9) assumes that there is a linear relationship between the  $\ln K_c$  and  $1/T$ . The thermodynamic parameters tabulated using this equation is given in Table III.

It has been reported that negative values of  $\Delta G^{\circ}$  indicate spontaneous adsorption while positive values mean that the adsorption process is nonspontaneous.<sup>22</sup> According to Errais et al.<sup>22</sup> negative values of  $\Delta G^{\circ}$  indicate that the adsorption process is thermodynamically feasible. In that regard, the  $\Delta G^{\circ}$  values in Table III mean that the adsorption of Pb(II) on the C20A-PCL composites is not thermally feasible in the temperature range used. In our

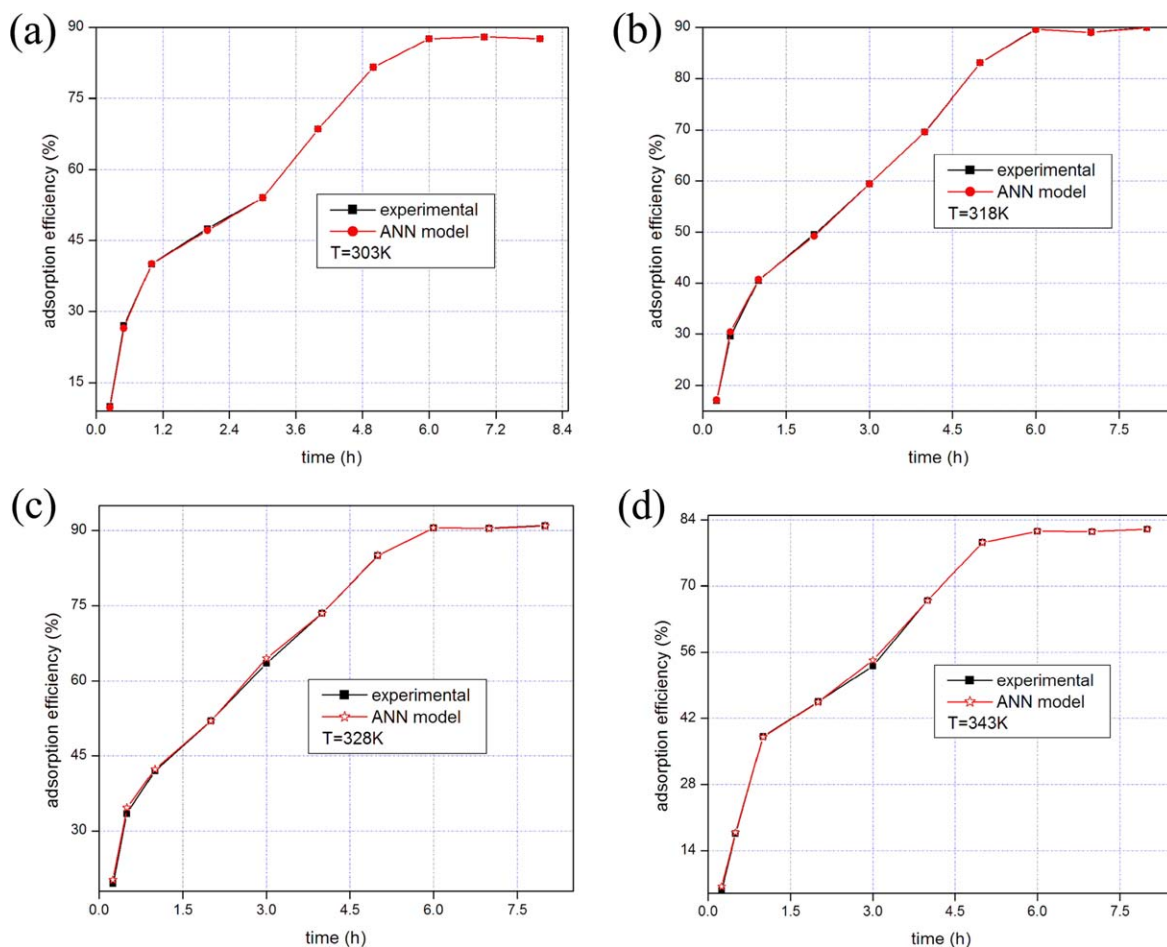


**Figure 7.** Effect of temperature on the adsorption of Pb(II) at pH 5.5, and  $C_0 = 200 \text{ mg/l}$ . [Color figure can be viewed in the online issue, which is available at [wileyonlinelibrary.com](http://wileyonlinelibrary.com).]

previous work on bentonite/polymer blend composites it was found that the adsorption of Pb(II) is thermally feasible at 293 K.<sup>23</sup> The observed increase in the adsorption efficiency with an increase in temperature (from 313 to 323 K) could be due to the enhanced mobility of adsorbate molecules rather than thermodynamic feasibility.  $\Delta G^0$  can also be used to predict the adsorption mechanism. Adsorption of heavy metals can occur through chemisorption, physisorption, or ion-exchange. Sölener et al.<sup>24</sup> stated that  $\Delta G^0$  for physical adsorption ranges between the magnitudes of 20 and 0 kJ mol<sup>-1</sup> and generally range between 20 and 80 kJ mol<sup>-1</sup> in cases of coexistence of chemisorption and physisorption. The  $\Delta G^0$  values shown in Table III show that the adsorption of Pb(II) was mostly through the coexistence of chemical and physical adsorption.

Just like  $\Delta G^0$ , the magnitude of  $\Delta H^0$  could be used to predict the dominant mechanism involved in the adsorption process, i.e. chemical or physical interactions. Adsorption enthalpies over the range of 80 and 420 kJ mol<sup>-1</sup> signify electrostatic adsorption. Rahmani et al.<sup>21</sup> reported that an enthalpy of less than 80 kJ mol<sup>-1</sup> indicates that the adsorption involves physisorption. According to Li et al.<sup>25</sup> the physical adsorption with an enthalpy in the range of 4 and 8 kJ mol<sup>-1</sup> indicates Van Der Waals interactions, whereas in the range of 8 and 40 kJ mol<sup>-1</sup> hydrogen bonding is the main interaction. As can be seen from Table III, the removal of Pb(II) in the present study was mostly through hydrogen bonding between the bentonite and the adsorbate suggesting that the adsorbed metal was hydrated. This finding makes sense because at pH 5.5 Pb(II) may exist as Pb(OH)<sup>+</sup>. The negative  $\Delta S^0$  values signify that there is a decrease in the randomness at the composite—Pb(II) solution interface.<sup>22,26</sup>

## CONCLUSIONS

An ANN model has been successfully developed for the prediction of the adsorption efficiency of Pb(II) from water using clay-polymer composites fabricated via the melt-blending technique. The model was to predict the effect of pH, contact time, and temperature on the removal of Pb(II) from water by a C20A-PCL composite. The correlation was outstanding. Pertaining to the composite performance, it was remarkable to note that with a filler content of 3% (w/w), it could remove 87% Pb(II) from water, yet it is 0.5 mm thick. Thermodynamic studies revealed that the uptake of Pb(II) from water using the clay-polymer adsorbents was not favorable at temperatures ranging between 303 and 328 K. The findings of this research are expected to stimulate renewed interest in adsorption as a method for water treatment. To date, the application of adsorption in water-treatment systems has been hindered by the problems posed by using the powder adsorbents. Such problems include incomplete recovery of the adsorbent after the adsorption process.

## ACKNOWLEDGMENTS

The authors would like to extend their sincere gratitude to Mr Dumisani Ndzinisa (M.Sc. student in the Mathematics Department, University of Johannesburg) and Mr John Kabuba (Ph.D. student in the Metallurgy Department, University of Johannesburg) for fruitful discussions on ANN. The University of Johannesburg (UJ) is acknowledged for funding this project.

## REFERENCES

1. Kul, A. R.; Koyuncu, H. *J. Hazard. Mater.* **2010**, *179*, 332.
2. Liu, Y.; Liu, Z.; Gao, J.; Dai, J.; Han, J.; Wang, Y.; Xie, J.; Yan, Y. *J. Hazard. Mater.* **2011**, *186*, 197.
3. Mishra, B.; Haack, E. A.; Maurice, P. A.; Bunker, B. A. *Chem. Geol.* **2010**, *275*, 199.
4. Passos, C. G.; Ribaski, F. S.; Simon, N. M.; dos Santos, A. A. Jr.; Vaghetti, J. C. P.; Benvenutti, E. V.; Lima, É. C. *J. Colloid Interface Sci.* **2006**, *302*, 396.
5. Sheng, G.; Wang, S.; Hu, J.; Lu, Y.; Li, J.; Dong, Y.; Wang, X. *Colloid Surf A: Physicochem. Eng. Aspects* **2009**, *339*, 159.
6. Xu, D.; Tan, X. L.; Chen, C. L.; Wang, X. K. *Appl. Clay Sci.* **2008**, *41*, 37.
7. Zou, W.; Han, R.; Chen, Z.; Jinghua, Z.; Shi, J. *Colloid Surf. A: Physicochem. Eng. Aspects* **2006**, *279*, 238.
8. Dlamini, D. S.; Mishra, A. K.; Mamba, B. B. *Mater. Chem. Phys.* **2012**, *133*, 369.
9. Dlamini, D. S.; Mishra, A. K.; Mamba, B. B. *J. Inorg. Organomet. Polym. Mater.* **2012**, *22*, 342.
10. Motsa, M. M.; Thwala, J. M.; Msagati, T. A. M.; Mamba, B. B. *Phys. Chem. Earth* **2011**, *36*, 1178.
11. Mthombo, T. S.; Mishra, A. K.; Mishra, S. B.; Mamba, B. B. *J. Appl. Polym. Sci.* **2011**, *121*, 3414.
12. Dlamini, D. S.; Mishra, A. K.; Mishra, S. B.; Mamba, B. B. *J. Inorg. Organomet. Polym. Mater.* **2011**, *21*, 229.
13. Dlamini, D. S.; Mishra, A. K.; Mishra, S. B.; Mamba, B. B. *J. Comput. Mater.* **2011**, *45*, 2211.
14. Paczkowska, B.; Strzelec, S.; Jedrzejewska, B.; Linden, L.-A.; Paczkowski, J. *Appl. Clay Sci.* **2004**, *25*, 221.
15. Elemen, S.; Kumbasar, E. P. A.; Yapar, S. *Dyes Pigments* **2012**, *95*, 102.
16. Yetilmezsoy, K.; Demirel, S. *J. Hazard. Mater.* **2008**, *153*, 1288.
17. Giri, A. K.; Patel, R. K.; Mahapatra, S. S. *Chem. Eng. J.* **2011**, *178*, 15.
18. Ghandehari, S.; Montazer-Rahmati, M. M.; Asghari, M. *Desalination* **2011**, *277*, 348.
19. Turana, N. G.; Mescib, B.; Ozgonenel, O. *Chem. Eng. J.* **2011**, *171*, 1091.
20. Vieira, M. G. A.; Neto, A. F. A.; Gimenes, M. L.; da Silva, M. G. C. *J. Hazard. Mater.* **2010**, *176*, 109.
21. Rahmani, A.; Mousavi, H. Z.; Fazli, M. *Desalination* **2010**, *253*, 94.
22. Errais, E.; Duplay, J.; Darragi, F.; M'Rabet, I.; Aubert, A.; Huber, F.; Morvan, G. *Desalination* **2011**, *275*, 74.
23. Dlamini, D. S.; Mishra, A. K.; Mamba, B. B. *J. Appl. Polym. Sci.* **2012**, *124*, 4978.
24. Sölener, M.; Tunali, S.; Özcan, A. S.; Gedikbey, A. T. *Desalination* **2008**, *223*, 308.
25. Li, L.; Liu, F.; Jing, X.; Ling, P.; Li, A. *Water Res.* **2011**, *45*, 1177.
26. Wang, Q.; Chan, X.; Li, D.; Hu, Z.; Li, R.; He, Q. *J. Hazard. Mater.* **2011**, *186*, 1076.